Agricultural and Forest Meteorology 307 (2021) 108508

Contents lists available at ScienceDirect

Agricultural and Forest Meteorology

journal homepage: www.elsevier.com/locate/agrformet

Impacts of juniper woody plant encroachment into grasslands on local climate

Jie Wang [a,b], Xiangming Xiao [a,*], Jeffrey Basara [c,d], Xiaocui Wu [a], Rajen Bajgain [a,e], Yuanwei Qin [a], Russell B. Doughty [a], Berrien Moore III [f]

[a] Department of Microbiology and Plant Biology, University of Oklahoma, Norman, OK 73019, United States
[b] College of Grassland Science and Technology, China Agricultural University, Beijing 100094, China
[c] School of Meteorology, University of Oklahoma, Norman, OK 73019, United States
[d] Oklahoma Climate Survey, Norman, OK 73019, United States
[e] Sustainable Water Management Research Unit, USDA Agricultural Research Service, Stoneville, Mississippi, United States
[f] College of Atmospheric and Geographic Science, University of Oklahoma, Norman, OK, 73019, United States

ARTICLE INFO

Keywords:
Land cover
Land surface temperature
Evapotranspiration
Surface energy balance
Biological invasions

ABSTRACT

Woody plant encroachment (WPE) into grasslands has been exacerbated by climate change and human activities. WPE may affect local climate by altering the exchange of mass and energy between the land surface and the atmosphere. The lack of studies on the effects of WPE on local climate hinders our understanding of the interactions between changes in regional vegetation cover and climate. Here, we analyzed the differences of land surface temperature (ΔLST), albedo (ΔAlbedo) and evapotranspiration (ΔET) between juniper-woody-encroached grasslands and adjacent pure grasslands using 16-years of remote sensing data. Our results showed that juniper woody plant encroachment (JWPE) into the semi-arid and sub-humid grasslands reduced daytime LST and albedo, but increased nighttime LST and ET from an annual scale analysis. With each one percent increase in juniper cover, annual mean daytime ΔLST decreased ~0.026 °C, nighttime ΔLST increased ~0.01 °C, daily ΔLST decreased ~0.008 °C, Δalbedo decreased ~0.053%, and ΔET increased ~1.31 mm/year. Furthermore, it is suggested that the impacts of JWPE on LST and ET were stronger in dry years than in normal and pluvial years, and that no significant variations in albedo were found among the different hydrological conditions. These results provide insights into applying satellite-based techniques to understand the feedbacks between woody vegetation dynamics and local climate change.

1. Introduction

Woody plant encroachment (WPE) has relative mixing ratios of herbaceous and woody plants in grasslands and savannas around the world (Archer, 2010; Saintilan and Rogers, 2015). These ecological community transitions have been accelerated by human activities and climate change over the last 150 years (Archer et al., 1994; Wilcox and Huang, 2010). WPE has extensive ecological and socioeconomic implications by altering the soil-plant-atmosphere system, biophysical processes, and ecosystem services (Huxman et al., 2005; Petrie et al., 2015; Scott et al., 2014). In particular, WPE can affect regional climate by altering the fluxes of energy, water and momentum between the land surface and atmosphere (Bonan et al., 2003; Foley et al., 2005). However, to date, few studies that used climate models (Bonan, 1997, 1999) and satellite observations (Alkama and Cescatti, 2016; Li et al., 2015; Ma et al., 2017; Peng et al., 2014) have incorporated the climate impacts of this worldwide land surface change from WPE.

WPE is assumed to modify the land surface biophysical characteristics (Ge and Zou, 2013; He et al., 2015). In terms of the biophysical differences between pure grasslands (PG) and juniper woody plant encroached (JWPE) grasslands, juniper trees have a higher leaf area index (LAI) than grasses, which may increase the interception of rainfall (Wilcox, 2002). Deep-rooted juniper trees can extract deeper soil water than grasses, which can affect ecohydrological functions (Huxman et al., 2005; Scott et al., 2014). Juniper trees, an evergreen species, are darker than grasses, which leads to lower albedo and more absorption of solar radiation (Betts and Ball, 1997; Nair et al., 2007). Furthermore, WPE in grasslands increases the roughness of the land surface, which causes

* Corresponding author.
E-mail address: xiangming.xiao@ou.edu (X. Xiao).

https://doi.org/10.1016/j.agrformet.2021.108508
Received 26 May 2020; Received in revised form 6 June 2021; Accepted 7 June 2021
Available online 24 June 2021

enhanced turbulence between the land surface and the atmosphere (Ge and Zou, 2013). WPE can also shade out other vegetation and cause increased bare soil fraction, which can increase the ground heat fluxes during the daytime (Ge and Zou, 2013; He et al., 2015). The effects of land cover change on surface temperature is determined mainly by two critical biophysical mechanisms: albedo and evapotranspiration (ET) (Gibbard et al., 2005; Ma et al., 2017). Reduced albedo from JWPE tends to create a warming effect on the local climate. Conversely, increased LAI, root depth, and surface roughness could promote ET and cool the land surface. Albeit WPE has the potential to alter the biophysical attributes of grassland ecosystems and affect the interactions between land surface and climate, the changes in land surface temperature (LST), albedo, and ET in grasslands after WPE have not been examined widely, yet.

Previous studies paid more attention to the impacts of abrupt land cover change (LCC) on climate at regional and global scales using model-based analyses (Findell et al., 2017; Ma et al., 2017; Pitman et al., 2009). Meanwhile, the model-based analyses showed significant uncertainties which mainly stem from the representation and parameterization of biophysical variables (e.g. evapotranspiration, albedo) and descriptions of land cover change (Ma et al., 2017; Oleson et al., 2004; Pitman et al., 2009). For example, in the temperate mid-latitude zone, some simulations suggested that the conversions of forest to croplands or pastures led to a cooling effect driven by increased albedo (Bonan, 1999; Davin and de Noblet-Ducoudre, 2010), but others reported a warming effect due to reduced evapotranspiration (Findell et al., 2009; Malyshev et al., 2015). Uncertainties were also found in a JWPE associated study that examined the climate impacts of eastern redcedar (*Juniperus virginiana*) encroachment in the Southern Great Plains, USA, using a regional atmospheric modeling system (RAMS) (Ge and Zou, 2013). As suggested in the study, the main biophysical parameters (e.g., albedo, LAI) used in the RAMS model were difficult to verify due to the difficulties of obtaining the samples of such parameters and describing the eastern redcedar encroachment patterns at large spatial scales (Ge and Zou, 2013). Satellite observations provide direct information on the biophysical variables and land-use/land-cover dynamics, which sheds new insights on the climate effects of abrupt LCC at regional and global scales (Alkama and Cescatti, 2016; Findell et al., 2017; Peng et al., 2014). WPE is a form of ecological succession and occurs over many decades which differs from the abrupt land-cover change, for example, afforestation and deforestation (Jackson et al., 2007). Few studies have been carried out to quantify the WPE effects on temperature, ET and albedo by data-driven approaches based on in-situ or satellite observations. These observation-based assessments can provide references for studies on incorporating such large-scale ground change from WPE into climate and vegetation dynamic models and reducing the simulation uncertainties (Alkama and Cescatti, 2016; Findell et al., 2017; Peng et al., 2014).

Previous studies concentrated on the local climatic effects of deforestation and afforestation, which is treated separately from WPE in continental-scale C budgets (Barger et al., 2011). The previous results suggested that temperature responses to vegetation type change are dependent upon a precipitation gradient and a latitudinal gradient at a global scale (Foley et al., 2003; Li et al., 2015; Peng et al., 2014; Snyder et al., 2004), but little attention has been given to the climatic effects of WPE despite its global extent. In particular, the roles of woody plants in regulating climate in the semi-arid areas within the temperate mid-altitude zone are largely uncertain Bonan (2008), Li et al. (2015), Peng et al. (2014). It is especially unclear if interannual variability of precipitation influences the temperature responses to woody plant change within a specific region.

Juniper are widely distributed conifer woody species (Meneguzzo and Liknes, 2015). Juniper encroachment in the native grasslands and shrublands has been reported as one of the pronounced ecosystem changes in the Great Plains and the western United States in recent years (Barger et al., 2011; Meneguzzo and Liknes, 2015; Sankey and Germino, 2008). In this study, our overall goal is to understand the impacts of JWPE on local LST, albedo and ET within the grasslands in semi-arid and sub-humid temperate regions based on satellite observations. Specifically, we aim to: (1) examine the differences in LST (ΔLST), albedo (ΔAlbedo) and ET (ΔET) between juniper-encroached grasslands (JEGs) and adjacent pure grasslands (PGs) at annual and seasonal scales; (2) characterize the relationships between ΔLST, ΔAlbedo, ΔET and the proportion of JWPE in landscapes; and (3) examine how the effects of JWPE on local climate vary with different hydrological years (dry, normal and pluvial years). The grasslands in the state of Oklahoma, USA, were selected as a study area because they are in a temperate mid-altitude zone with a semi-arid and sub-humid climate, and have experienced extensive JWPE (*Juniperus* spp.) over the last several decades (Engle et al., 1996; Wang et al., 2017, 2018a).

2. Material and methods

2.1. Study area

The grasslands in Oklahoma (33.4°N ~ 37.1°N, 94°W ~ 103.2°W), USA, are characterized by various grass types including shortgrass, mixed-grass, and tallgrass from the western to eastern regions (Hoagland, 2000). In recent years, the abundance of various juniper species, such as Eastern redcedar (*J. virginiana*) and Ashe juniper (*J. ashei*), has been increasing in grasslands (Engle et al., 1996). The grasslands are in a temperate continental climate with annual mean air temperature of 13–17 °C from north to south and annual mean precipitation of ~400–1100 mm from west to east. A majority of JWPE occurred in the grasslands with annual mean precipitation of ~600–1100 mm and elevation ranging from ~200-m to ~500-m (Figs. 1, 2).

2.2. Data

2.2.1. Land cover maps

We have developed a workflow to generate 30-m juniper forest encroachment maps for Oklahoma using a pixel and phenology-based algorithm from the Phased Array type L-band Synthetic Aperture Radar (PALSAR) in 2010 and time series Landsat images during 1984–2010 (Wang et al., 2017, 2018a). In this study, we used the same approach to generate the 30-m juniper forest encroachment map for the period of 2011–2015 using the follow-on SAR (PALSAR-2) data in 2015 and time series Landsat images during 2011–2015. Four main steps were included in this workflow (Wang et al., 2017, 2018a).We first generated the forest map in 2015 using the PALSAR-2 images and the decision rule of $16 < HV < -8$, and $2 < HH—HV < 8$, and $0.3 < HH/HV < 0.85$ (Fig. S1b). Then, the annual evergreen forest maps during 2011–2015 were generated using the Land Surface Water Index (LSWI) by a frequency of LSWI>0 larger than 0.9 in each year. Based on the annual evergreen forest maps, we continued to map the annual juniper forest distribution using the Normalized Difference Vegetation Index (NDVI) by the decision rule of mean NDVI in winter season larger than 0.4. Finally, these annual juniper forest maps were combined to generate the juniper forest encroachment map for the period of 2011–2015 by a frequency combination approach, which extracted the pixels with a frequency $\geq$ 50% identified as juniper forests during the study period of 2011–2015.

In this workflow, the 25-m PALSAR and PALSAR-2 mosaic data were acquired from the Earth Observation Research Center, Japan Aerospace Exploration Agency (JAXA), having HH and HV polarization bands (Shimada et al., 2014). The developed algorithms based on PALSAR and PALSAR-2 datasets can produce high quality forest and evergreen forest maps with overall accuracies around 95% or higher (Chen et al., 2018; Qin et al., 2016). This workflow has been evaluated using ground truth data and very-high-resolution observations and it generated the juniper forest encroachment maps with an overall accuracy of ~96%, producer's accuracy of ~89% and user's accuracy of ~95% (Wang et al.,

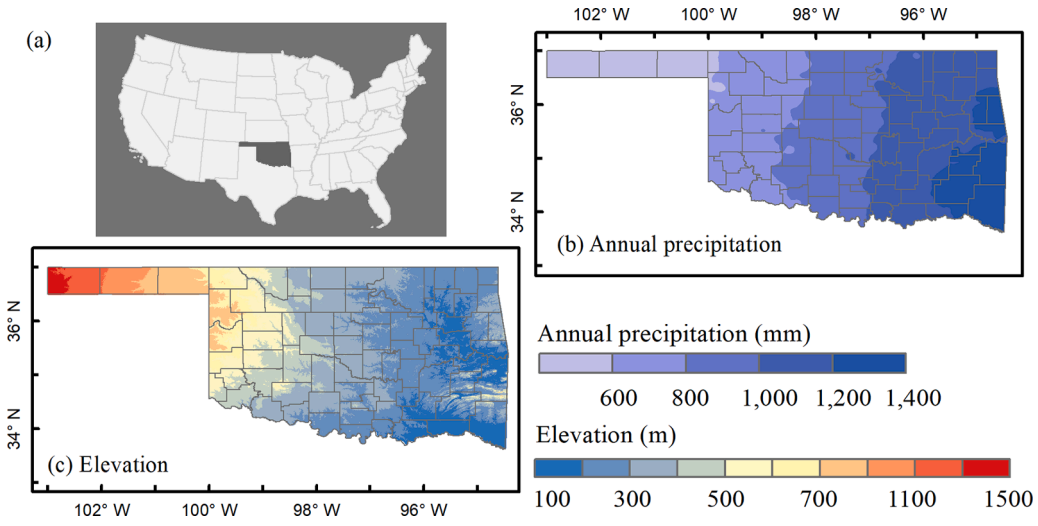

Fig. 1. The location, climate and elevation of Oklahoma. (a) the location of Oklahoma state, USA; (b) the annual precipitation gradient in Oklahoma from the Parameter-elevation Relationships on Independent Slopes Model (PRISM) 800-m precipitation datasets in 1980–2010 (http:// prism.oregonstate.edu/); (c) the elevation distribution from the 30-m Shuttle Radar Topography Mission Digital Elevation Model (SRTM/DEM).

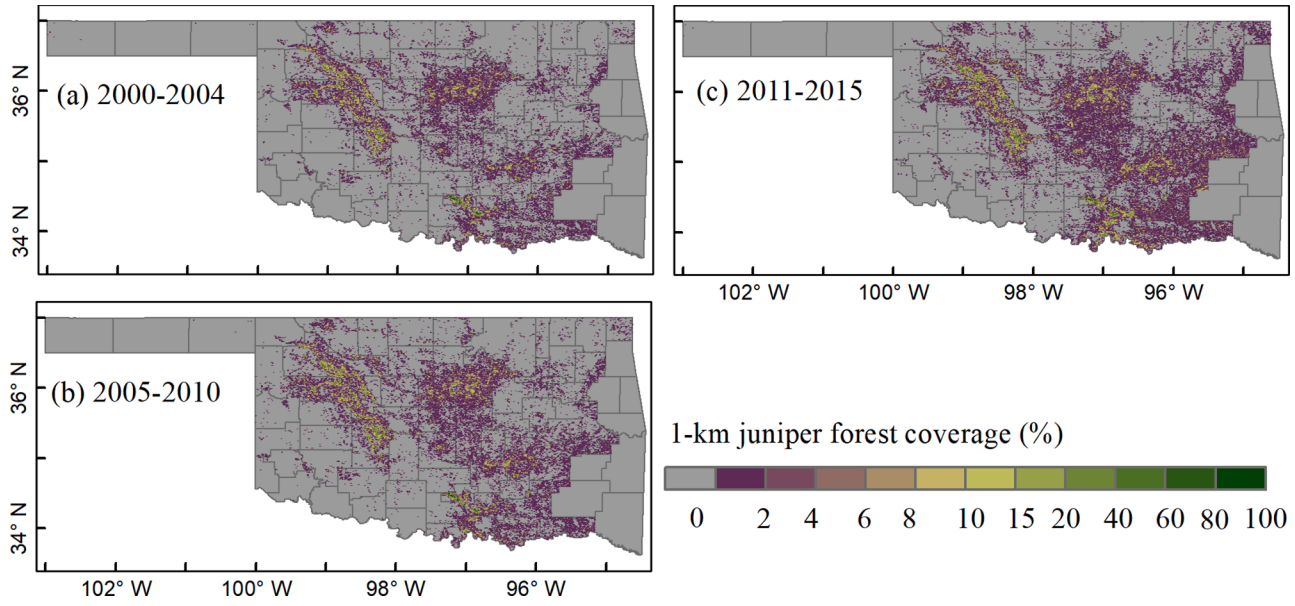

Fig. 2. Spatial distribution of juniper forest coverage for the three periods of (a) 2000–2004, (b) 2005–2010, and (c) 2011–2015 in Oklahoma, USA.

2017, 2018a, 2018b). More details on the mapping materials and methods have been published in our previous works (Chen et al., 2018; Qin et al., 2016; Wang et al., 2017, 2018a).

To match the timeline of Moderate-Resolution Imaging Spectroradiometer (MODIS)-based datasets, we selected the juniper forest encroachment maps for three periods, the early 2000s (2000–2004), the late 2000s (2005–2010), and the early 2010s (2011–2015). Then, these 30-m juniper forest binary (juniper or non-juniper forests) maps were aggregated to 1-km juniper forest coverage (JFC,%) maps to match the spatial resolution of the MODIS land surface temperature data (Fig. 2). In addition, the produced 25-m forest maps in 2010 and 2015 were used to show the distributions of non-juniper forests in the following analysis (Fig. S1a,b). These 25-m forest maps were also aggregated to 1-km as forest coverage (%) maps.

Annual MODIS land cover data at 500 m spatial resolution (MCD12Q1, Collection-6) were used to describe the grassland distribution during 2001–2015. We just selected the grassland pixels from the land cover classes to generate the annual 500-m grassland maps. These 500-m binary grassland maps were then aggregated to 1-km grassland coverage (%) maps. Finally, we produced the 1-km grassland maps by selecting the pure pixels with persistent 100% grassland cover in each period based on the annual 1-km grassland coverage maps (Fig. S1c,d,e). These 1-km grassland maps were binary with values of 1 and 0 to present 1-km pixels with pure grassland cover or not during a given study period of 2000–2004, 2005–2010, and 2011–2015.

2.2.2. *Land surface temperature (LST) data*

We used MODIS LST products from Terra (MOD11A2, Collection-6) from 2000 to 2015 and Aqua (MYD11A2, Collection-6) from 2002 to 2015. The daytime and nighttime LST were provided at ~10:30 am and ~22:30 pm local solar time from MOD11A2 and ~13:30 pm and ~1:30 am local solar time from MYD11A2. The LST data have a 1-km spatial resolution and 8-day temporal resolution. The absolute errors were evaluated to be less than 1 K (Wan, 2014). The pixels with valid quality were used in this study (Table S1, Fig. S2).

2.2.3. Albedo datasets

The daily MODIS albedo products (MCD43A3, Collection-6) were available at 500-m spatial resolution and provided black-sky and white-sky albedos for seven spectral bands and three broad bands (Schaaf and Wang, 2015). This latest albedo product was validated using globally-distributed tower measurements and has the ability to capture land surface dynamics. The broadband shortwave blue-sky albedo had a root-mean-square error (RMSE) of less than 0.0318. The blue-sky albedos can be calculated as the average of black-sky and white-sky albedos assuming equal contributions from direction illumination and diffuse illumination as done in previous studies (Li et al., 2015; Ma et al., 2017). We used all the valid albedo values to generate the blue-sky albedo at the shortwave broadband (0.3–5.0 μm) from 2000 to 2015 (Table S1). The average annual mean blue-sky albedo for each period were shown in Fig. S3a,c,e.

2.2.4. Evapotranspiration (ET) datasets

We acquired the 500-m MODIS 8-day (MOD16A2, Collection-6) ET products for 2001–2015. These datasets were produced using an improved ET algorithm from the Penman-Monteith model based on MODIS reflectance and meteorological reanalysis data (Mu et al., 2013, 2011). It is a widely used satellite-based product in water cycle studies (Peng et al., 2014; Spera et al., 2016). The average mean absolute bias (MAE) of daily ET was 0.33 mm/day when compared to eddy flux towers (Mu et al., 2013; Running et al., 2017). The MAEs for grasslands and woody savanna were reported as 0.28 and 0.19 mm/day, respectively. The good quality data was used following the descriptions of the quality control layer (Table S1, Fig. S3b,d,f).

2.2.5. Climate data

Annual precipitation (AP) for 2000–2015 were obtained from Oklahoma Mesonet observations (Brock et al., 1995). The measurements from 77 Mesonet stations located at the juniper encroachment regions were averaged to show the annual precipitation in the study area (Fig. S4a). Then, the mean and standard deviation (STDEV) of annual precipitation during 2000–2015 were calculated to classify the dry (AP $<$ mean - STDEV), normal (mean - STDEV $<$ AP $<$ mean + STDEV), and pluvial (AP $>$ mean + STDEV) years. During 2000–2015, the mean annual precipitation was about 853 mm with a STDEV of 195 mm (Fig. S4b). There were two dry years, 2011 (610 mm) and 2012 (648 mm), and two pluvial years of 2007 (1120 mm) and 2015 (1351 mm). The remaining years were classified as normal years with a mid-distribution of annual precipitation. This STDEV method has been frequently used to determine drought and pluvial events (Christian et al., 2015).

2.3. Methods

2.3.1. Pairwise comparison of LST, albedo and ET between juniper-encroached grasslands and pure grasslands

Pairwise comparison is an approach commonly used to assess differences in ecological, hydrological, and climate factors under different land cover types (Lee et al., 2011; Ma et al., 2017; Peng et al., 2014). We used this approach to examine the differences in LST, ET, and albedo between the juniper-encroached grasslands (JEG) and adjacent pure grasslands (PG) over three periods of 2000–2004, 2005–2010, and 2011–2015 (Fig. 3). JEG pixels had a varying percentage of juniper forest at a given spatial resolution in contrast to PG pixels, which were 100% grassland. The JEG and adjacent PG samples were selected following the rules adopted in our recent study (Wang et al., 2018b): (1) the JEG samples should have relatively significant juniper forest cover; and (2) the adjacent PG samples should be covered by pure grasslands. The neighborhood window sizes were determined using two factors: (1) there were at least 10% of the PG pixels in the neighborhood of a JEG pixel, and (2) the window size should reduce the influence of spatial heterogeneity (Wang et al., 2018b). Thus, we used two neighborhood windows of 5 by 5 pixels (~5 by 5-km) and 11 by 11 pixels (~11 by 11-km) to select the adjacent PG pixels around a given JEG pixel following our previous study (Wang et al., 2018b). These PG pixels show the grasses between juniper woody trees.

At 1-km spatial resolution, the JFC maps, forest coverage maps, and grassland binary maps (grassland or non-grassland) were used to select JEG pixels only composed of juniper forests and grasslands without the cover of non-juniper forests. To select the pixels with significant JWPE, we used the JEG pixels having at least 10% juniper forest cover for all the periods of 2000–2004, 2005–2010, and 2011–2015 (Fig. S5). Using these JEG pixels, we used neighborhood windows of 5 by 5 pixels and 11 by 11 pixels to select adjacent PG pixels to construct pair samples. The JEG pixels having at least 10% adjacent PG pixels in their neighborhood were used for pairwise comparison analysis (Fig. S6). At last, the numbers of selected JEG pixels for three periods were 653, 757, and 1027 using 5 by 5 neighborhood window and 742, 829, and 1387 using 11 by 11 neighborhood window, respectively (Fig. S6). These selected JEG samples for three periods had an average juniper forest coverage of about 19% (Fig. S6). Using these JEG samples, we built comparison pairs between each JEG sample and the mean status of its adjacent PG pixels pair which was used in the following pairwise comparison analysis of LST, ET and albedo expressed as Eqs.(1)–(3).

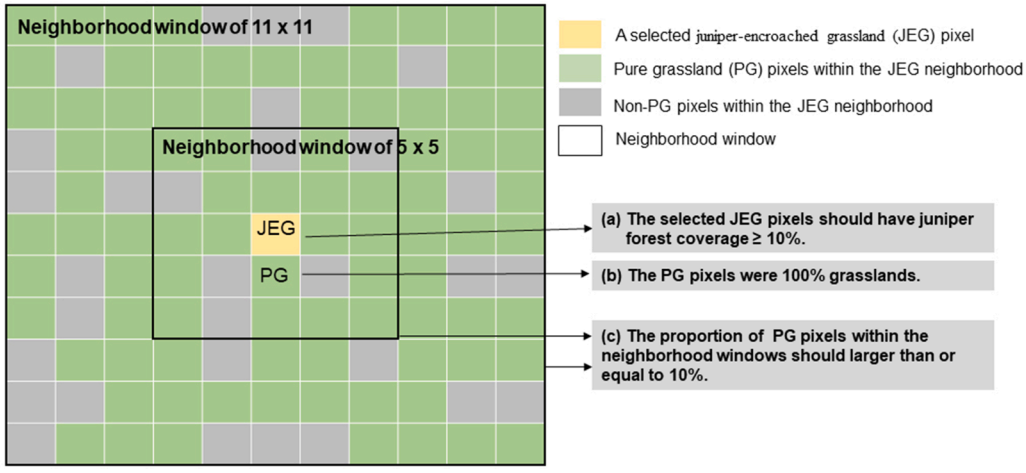

Fig. 3. A schematic figure is used to show the pairwise comparison approach used in this study. This approach was used to quantitatively assess the differences in LST, ET and albedo between the juniper-encroached grasslands (JEG) and adjacent pure grasslands (PG). To construct the JEG and PG pairs, we used the 1-km juniper forest coverage maps, forest coverage maps, and grassland maps to select the JEG and PG pixels. The JEG pixels were selected from the juniper forest coverage maps with conditions of (a) the juniper forest coverage should be larger than or equal to 10% and (b) the proportion of PG pixels within their neighborhood windows (5 by 5 or 11 by 11 pixels) should be larger than or equal to 10%. Thus, after averaging the PG pixels in each neighborhood window, we obtained a JEG and PG comparison

within a 5 by 5 and a 11 by 11 neighborhood window. Fig. S7 shows the distributions of the selected JEG pixels and adjacent PG pixels. As the 1-km juniper forest maps were used to select the JEG samples, the center distance of two adjacent JEG pixels are 1-km. These samples are mainly distributed in plain areas with elevation ranging from about 200-m to 500-m Figs. 1, S7). The JEG and PG samples were not filtered by elevation during the neighborhood analysis. In the pairwise comparison analysis of LST, we calculated the difference in LST (ΔLST) between the JEG pixel (LST_{JEG}) and the mean LST of the adjacent PG pixels (LST_{PG}) within each neighborhood window. This process is expressed as Eq. (1). The difference in LST shows the effects of juniper forest encroachment into grasslands on local land surface temperature. A positive or negative ΔLST represents the warming or cooling effect of juniper forest encroachment into grasslands, respectively. In this study, we calculated the daytime and nighttime LST as the mean values of Terra and Aqua observations. The daily LST was calculated as the mean values of daytime and nighttime LST. Similarly, we examined the differences in ET and albedo (ΔET and ΔAlbedo) between JEG and PG pixels. ΔET and ΔAlbedo is expressed as Eqs. (2) and ((3).

This pairwise comparison between JEG and PG pixels for LST, albedo, and ET was conducted at annual and seasonal time scales for three periods of 2000–2004, 2005–2010 and 2011–2015. The results assessed based on the 5 by 5-pixel sample window were shown in the main text, and those assessed based on the 11 by 11-pixel sample window were shown in supplementary materials.

$$\Delta LST = LST_{JEG} - LST_{PG} \quad \text{(Eq. 1)}$$

$$\Delta ET = ET_{JEG} - ET_{PG} \quad \text{(Eq. 2)}$$

$$\Delta Albedo = Albedo_{JEG} - Albedo_{PG} \quad \text{(Eq. 3)}$$

2.3.2. Quantitative relationships between the differences in LST, ET and albedo and the proportions of juniper forests

Higher percentages of juniper forest encroachment in the landscapes (pixels) were expected to result in larger changes in LST, albedo and ET (ΔLST, ΔAlbedo, andΔET). In this study, each sampling window for pairwise comparison had different proportions of juniper forest encroachment. Thus, we used simple linear regression models and the selected JEG samples in 2.3.1 to analyze the relationships between ΔLST, ΔET, ΔAlbedo, and the percent coverage of juniper forests. The results were presented by analyzing the samples together from the three study periods of 2000–2004, 2005–2010, and 2011–2015.

2.3.3. Impacts of hydrological conditions on the effects of juniper encroachment on LST, et and albedo

The changes in LST caused by land cover change have pronounced spatial patterns and are associated with precipitation magnitudes in space (Peng et al., 2014). We assumed that the differences in LST, albedo and ET between JEG and PG in a specific region may vary with the temporal dynamics of hydrological conditions. Therefore, we calculated ΔLST, ΔAlbedo, andΔET for the dry years (2011, 2012) and pluvial years (2007 and 2015) and then compared them with the average results calculated from the normal years in the study period of 2000–2015. The comparison among different hydrological conditions included annual ΔLST, ΔAlbedo, ΔET, and the relationships between ΔLST, ΔAlbedo, ΔET and the percentage of juniper forest cover.

3. Results

3.1. Effects of juniper forest encroachment on LST, albedo, and ET at annual scale

The differences in LST, albedo, and ET between JEGs and adjacent PGs grid cells (1-km resolution) were examined by pair-wise samples selected by 5 by 5 neighborhood windows (see *Methods*). JEGs had lower annual mean daytime LST (0.63±0.64 °C) and higher annual mean nighttime LST (0.16±0.41 °C) than did their adjacent PGs during the entire study period of 2000–2015 (mean difference±one standard deviation) (Fig. 4). At a daily scale with considering daytime and nighttime LST together, JEGs were assessed reducing mean annual daily LST by about 0.24±0.45 °C for the entire study period. For each of the three time periods, the average annual mean daytime LST for JEGs was lower by about 0.55±0.51 °C, 0.73±0.79 °C, and 0.64±0.65 °C in 2000–2004, 2005–2010 and 2011–2015, respectively (Fig. 4); average annual mean nighttime LST was higher by about 0.1 ± 0.40 °C, 0.2 ± 0.46 °C and 0.19±0.39 °C; and average annual mean daily LST was lower by about 0.23±0.41 °C, 0.26±0.48 °C and 0.23±0.39 °C. At the annual scale, juniper forest encroachment decreased albedo with a mean ΔAlbedo of approximately −1.5 ± 1%, and increased ET with mean ΔET of approximately 37±33 mm/year for 2000–2015 (Fig. 4). Consistent results were acquired using the samples selected by the 11 by 11 neighborhood window, despite slightly higher mean and standard deviation values for each variable (Fig. S8). Similar results were also obtained between the samples selected by the 5 by 5 and 11 by 11 neighborhood windows in the following *Sections of 3.2, 3.3 and 3.4* (Figs. S9–S11).

3.2. Effects of juniper forest encroachment on LST, albedo, and ET at seasonal scale

The seasonal dynamics of ΔLST during 2000–2015 show that juniper forest encroachment cools daytime surface temperature year-round (Fig. 5a). The cooling effect increased from January and reached a peak in the summer months, and then decreased around September (Fig. 5a). The juniper forest daytime cooling effect was stronger in spring and summer than in fall and winter (mean daytime ΔLST was −0.54±0.60 °C, −0.69±0.70 °C, −0.50±0.46 °C, and −0.43±0.42 °C from spring to winter, respectively). In contrast, the nighttime warming effect was stronger in winter and fall than in spring and summer (mean nighttimeΔLST was 0.18±0.25 °C, 0.13±0.22 °C, 0.22±0.31 °C, 0.28±0.38 °C from spring to winter, respectively). Throughout the year, the daytime cooling was stronger than the nighttime warming caused by JWPE (Fig. 5). These different climate effects for daytime and nighttime lead to a year-round cooling effects at the daily scale with more evident in spring and summer than in fall and winter (mean daily ΔLST of 0.18±0.24 °C, 0.28±0.32 °C, 0.14±0.18 °C, and 0.08±0.20 °C from spring to winter, respectively) (Fig. 5).

Seasonally, ΔAlbedo was high during the cold months from about November to the following February, while high ΔET occurred during the warm months from March to October (Fig. 5b,c). Winter had the highest ΔAlbedo (∼ −2.3 ± 1.5%) followed by fall (∼ −1.7 ± 1.1%), spring (∼ −1.5 ± 0.9%) and summer (∼ −1.4 ± 0.9%). Summer had the highest ΔET (about 2.5 ± 5.5 mm/month), followed by spring (about 2.1 ± 2.3 mm/month) and fall (about 2.0 ± 3.4 mm/month). The ΔET in winter was negligible (Fig. 5).

3.3. Relationships between changes in LST, albedo, ET, and juniper forest coverage (JFC,%)

There were significant negative ($P<0.001$) linear relationships between daytime ΔLST and JFC, which suggested about a 0.026 °C reduction in daytime ΔLST with one percent increase in JFC (OPI) (Fig. 6). Nighttime ΔLST rose with the increase of JFC with a rate of around 0.01 °C/OPI. Thus, a negative relationship was found between daily ΔLST and JFC (a rate of about −0.008 °C/OPI), which implied that the net effect of an increase in JFC caused lower daily LST.

Increasing JFC leads to opposite effects on ΔAlbedo and ΔET (Fig. 6). ΔAlbedo and JFC had a significant negative relationship ($P<0.001$) with a rate of about −0.053%/OPI. Significant positive linear relationships ($P<0.001$) were found between ΔET and JFC with a rate of about 1.31 mm/year/OPI. These JFC-based results supported the annual and seasonal analysis on the roles of juniper forest encroachment on ΔLST,

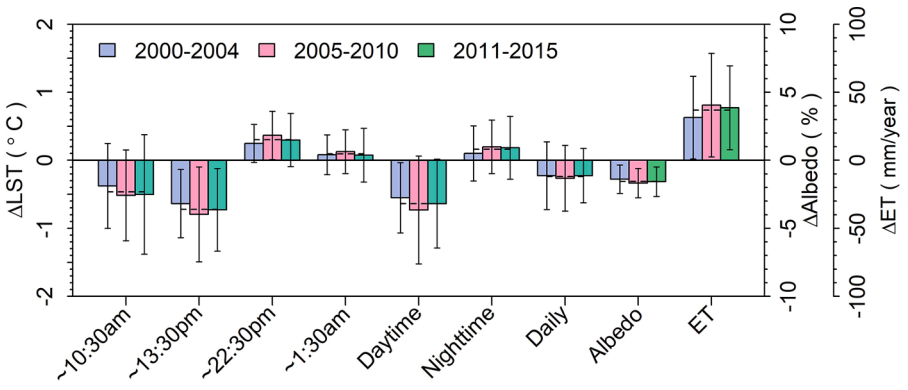

Fig. 4. Differences of land surface temperature (ΔLST), albedo (ΔAlbedo), and ET (ΔET) between juniper-encroached grasslands and adjacent pure grasslands. This figure shows the results for three periods of 2000–2004, 2005–2010, and 2011–2015. The dash lines present the average values of each variable over the three periods. This analysis used the annual mean LST in each period from MODIS Terra (~10:30am and ~22:30pm) and Aqua (~13:30pm and ~1:30am). The daytime LST was the mean LST at ~10:30 and ~13:30pm and the nighttime LST was the mean LST at ~22:30pm and ~1:30am. The daily LST was the mean LST of daytime and nighttime. The differences of all the examined variables are statically significant (P<0.001) between juniper-encroached grasslands and adjacent pure grasslands (Table S2).

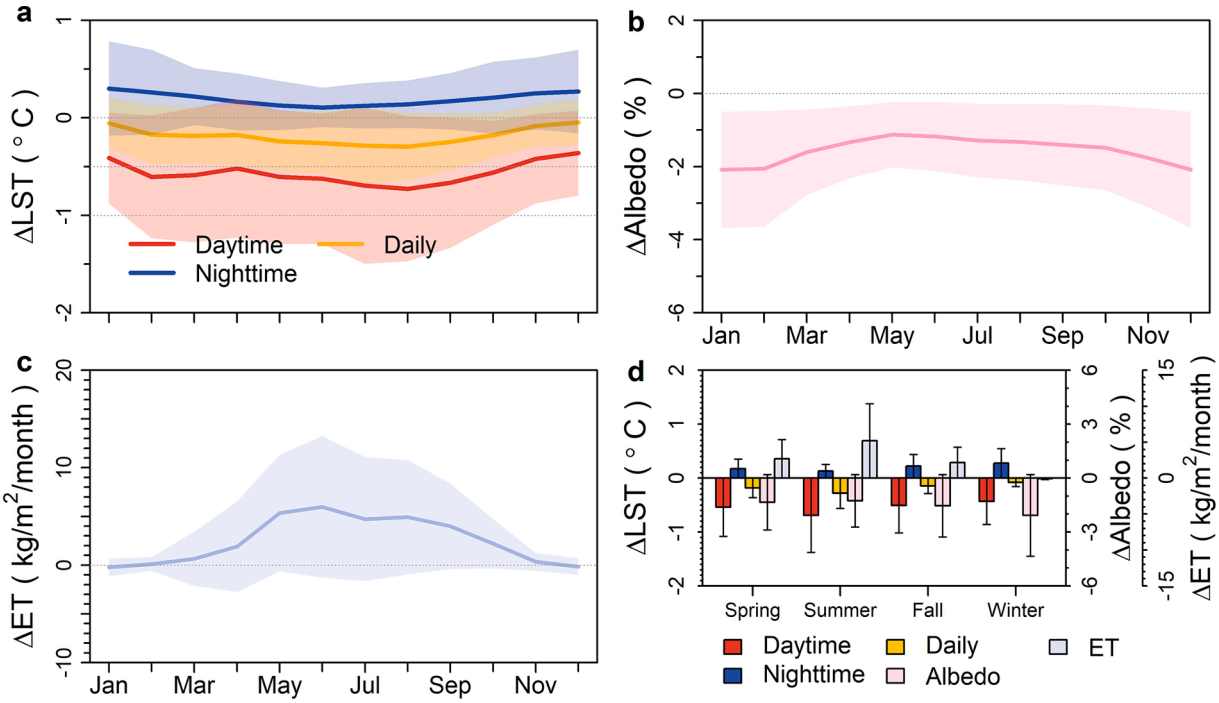

Fig. 5. Seasonal dynamics (a, b, c) and summary (d) of ΔLST, ΔAlbedo, and ΔET. The ΔLST, ΔAlbedo, and ΔET are the difference of each variable between juniper-encroached grasslands and adjacent pure grasslands during 2000–2015. The differences of all the examined variables are statically significant (P<0.05) between juniper-encroached grasslands and adjacent pure grasslands at monthly and seasonal scales (Tables S4-S5).

ΔAlbedo, and ΔET between JEGs and PGs.

3.4. Effects of juniper forest encroachment on LST, albedo, and ET in dry, normal, and pluvial years

JWPE reduced daytime LST and increased nighttime LST to a greater extent in dry years and less so in pluvial years (Fig. 7a). The net decrease of daily LST in dry years was also greater than that in pluvial years. From pluvial to dry cases, slight reduction was found in the decreased albedo caused by JWPE, while the effect of JWPE on ET was strengthened (Fig. 7a).The linear relationships (Figs. 7b,c, S12–S14) between daytime, nighttime, and daily ΔLST, ΔAlbedo, and ΔET and JFC agreed well with the findings based on multi-year statistical analysis in different hydrological conditions (Fig. 7a). From dry to pluvial years, the negative regression slopes increased between daytime, daily ΔLST, and JFC, and the positive regression slopes decreased between ΔET and JFC. No significant changes were founded in the regression slopes for nighttime ΔLST, ΔAlbedo, and JFC with different hydrological conditions.

4. Discussion

4.1. Factors controlling the effects of juniper forest encroachment on daytime and nighttime LST

Daytime LST is controlled by incoming solar radiation, land surface properties (e.g. topography, land cover, roughness, albedo and emissivity), and near-surface atmospheric boundary layer conditions, which alter the exchange of energy, water, and momentum balance between land surface and atmosphere (Foley et al., 2003; Peng et al., 2014; Zhou et al., 2012). The surface albedo decreased as juniper woody encroached into grasslands (Fig. 4), as trees tend to absorb more solar energy than grasses (Betts and Ball, 1997; Bonan, 2008). In surface energy balance system, net radiation is commonly partitioned as three fluxes: latent heat, sensible heat, and soil heat (Su, 2002). The surface cools through sensible heat loss caused by the wind and latent heat loss due to evapotranspiration (Foley et al., 2003). JWPE in grasslands increases the roughness and fragmentation of the land surface. The rougher surfaces increase air turbulence and enhance surface cooling through both

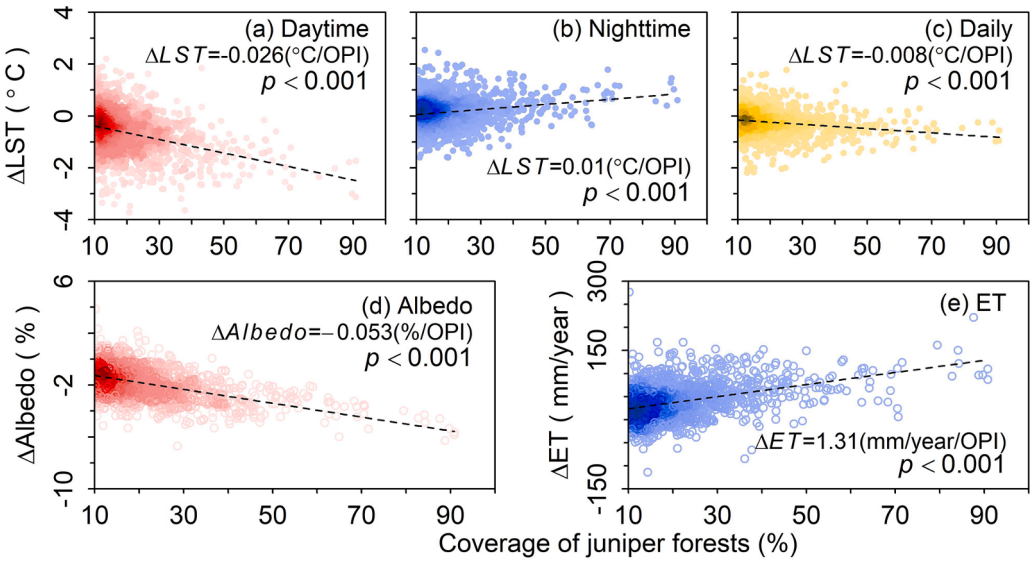

Fig. 6. Changes of ΔLST, ΔAlbedo, and ΔET with increasing juniper forest coverage. Relationships of (a, b, c) ΔLST in daytime, nighttime and daily, (d) ΔAlbedo, and (e) ΔET with coverage of juniper forests for 2000–2015 based on the data of three periods of 2000–2004, 2005–2010, and 2011–2015. OPI denotes one percentage increase in juniper forest coverage.

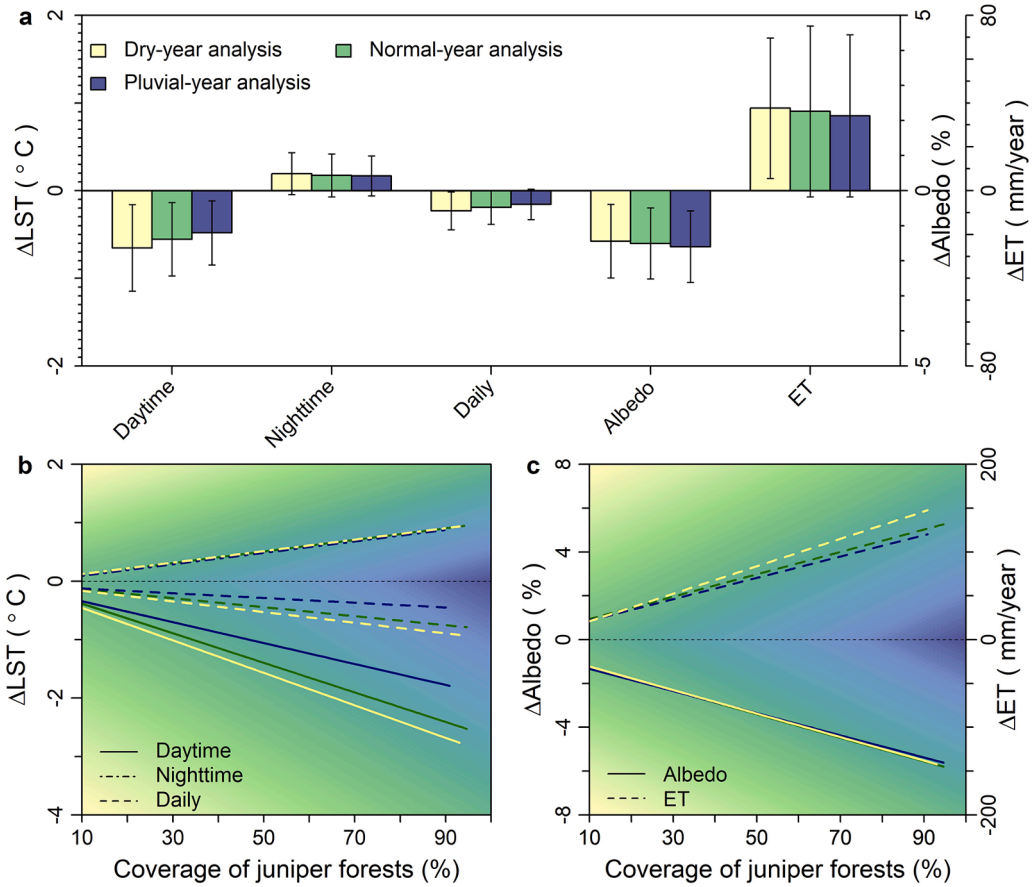

Fig. 7. Influence of hydroclimate on the effects of JWPE on LST, albedo, and ET. (a) Analysis of ΔLST, ΔAlbedo, and ΔET at dry, normal, and pluvial years. And the regression lines of (b) ΔLST in daytime, nighttime, and daily, (c) ΔAlbedo and ΔET with coverage of juniper forests for dry, normal, and pluvial years during 2000–2015. The regression analyses under each hydroclimate were shown in Figs. S12–S14.

sensible and latent heat loss (Foley et al., 2003; Ge and Zou, 2013; Juang et al., 2007). Juniper forests also have a higher leaf area index, a deeper root system, and thus have access to more water than grasslands due to the interception of precipitation in the canopy and access to deeper soil moisture (Huxman et al., 2005; Scott et al., 2014; Wang et al., 2018b). This water availability to juniper trees favors JWPE and explains the enhanced ET and decreased daytime LST in the juniper-encroached grasslands (Fig. 4).

Several mechanisms have been documented to explain the nighttime warming effects of woody plants encroachment, including the 'plant sheltering' effect, increased energy storage during the daytime, and the altered atmospheric boundary layer conditions (D'Odorico et al., 2010, 2013; He et al., 2010, 2011; Peng et al., 2014). At night, the heat exchange is determined by the long-wave radiation from the land surface (Geiger et al., 2009). Woody canopies can absorb part of the long-wave radiation and emit some back to the surface. This 'plant sheltering' effect could reduce the near surface cooling at night (Chen et al., 1993; Grimmond et al., 2000). Some observations found that WPE in grasslands increased the fraction of bare soil by reducing the understory herbaceous plants (D'Odorico et al., 2013; He et al., 2010). Thus, soils in WPE grasslands absorb more energy than in pure grasslands in the daytime, which causes higher nighttime surface temperature in WPE grasslands (D'Odorico et al., 2010; He et al., 2015, 2010, 2011). In addition, atmospheric boundary layer conditions contribute to the differences in the nighttime surface temperature of woodlands and grasslands (Geiger et al., 2009). For example, high daytime ET in woodlands increases the air humidity and cloud formation in the boundary layer, which prevents nighttime cooling relative to grasslands (Peng et al., 2014). Our results show that JWPE enhanced daytime ET, which might play some roles to the nighttime heat retention in the juniper-encroached grasslands.

4.2. Effects of juniper forest encroachment on LST at annual and seasonal scales

Our study suggested that the effects of JWPE on local climate were significant with average annual daytime cooling of about 0.026 °C and nighttime warming about 0.01 °C (mean of three study periods) with one percent increase in juniper cover. Although limited efforts have been done to quantify the impacts of WPE on local climate, the role of pure forests and non-forests (grasslands and croplands) in local climate has been studied using satellite observations, field measurements, and model simulations at global and regional scales (Findell et al., 2017; Lee et al., 2011; Liao et al., 2018; Ma et al., 2017; Peng et al., 2014). Previous satellite observations indicated that mean annual daytime LST in temperate forests were about 1.2 °C cooler than in surrounding croplands, and mean annual nighttime LST was about 0.45 °C warmer (Ma et al., 2017). Similarly, satellite-based studies in China reported that daytime LST was 1.1 °C lower in plantation forests than grasslands, and nighttime LST was 0.2 °C higher (Peng et al., 2014). In addition, a number of studies based on field observations have examined the ability of woody plants to modify the temperature regime within the canopy and at site and landscape scales (Chen et al., 1993; D'Odorico et al., 2013; Renaud et al., 2011; Renaud and Rebetez, 2009; Villegas et al., 2010). Lower maximum and higher minimum air temperatures have been observed in forest canopies in comparison to canopy gaps or adjacent grasslands (D'Odorico et al., 2013; Renaud et al., 2011; Renaud and Rebetez, 2009; Young and Mitchell, 1994). Other studies have also documented that the daytime cooling and nighttime warming effect of woody vegetation relative to contiguous grasslands across various woodland-grassland ecotones from boreal forests to arid and semi-arid woodlands (Alkama and Cescatti, 2016; D'Odorico et al., 2010; Findell et al., 2017; He et al., 2011; Langvall and Lofvenius, 2002; Li et al., 2015; Liao et al., 2018; Maher et al., 2005; Renaud and Rebetez, 2009; Voicu and Comeau, 2006). These findings confirmed our results about the interactions of woody plants and local environment in spite of the impacts of woody plants on local climate varying with tree species (Renaud and Rebetez, 2009).

Our results demonstrated that JWPE caused year-round daytime and daily cooling and nighttime warming. The daytime cooling effect was weaker in cold seasons (fall and winter) than in warm seasons (spring and summer), but the reverse was true for the nighttime warming effect (Fig. 5). Previous comparative studies reported similar seasonal dynamics in ΔLST between evergreen forests and nearby grasslands in temperate regions from flux and satellite data (Alkama and Cescatti, 2016; Liao et al., 2018; Zhao and Jackson, 2014). The seasonal dynamics of ΔAlbedo and ΔET that we observed in our study were consistent with the findings of a stronger ET in summer and lower albedo in winter for evergreen woodlands than grasslands (Betts and Ball, 1997; Zhao and Jackson, 2014). Increased roughness and deep roots of juniper species could explain the substantial enhancement of ET, which causes significant surface cooling happened in summer. Evergreen juniper species maintain a darker canopy than the dormant grasslands in winter (Wang et al., 2018b). It is associated with the larger difference in daytime solar radiation absorption and nighttime warming between JEGs and PGs during winter than in other seasons (Bonan, 2015).

4.3. Effects of juniper forest encroachment on LST under different hydrological conditions

We found that the cooling effect of JWPE on daytime and daily LST was more pronounced in dry years than in pluvial years. ΔET also varied with hydrological conditions, and we did not observe significant changes in albedo or nighttime LST. A similar observation was made in a previous study, which found that although surface temperatures and sensible heat flux increased in both forests and pastures during drought, pastures experienced a greater increase (9 °C) in surface temperature and forests had a greater sensible heat flux (Zaitchik et al., 2006). Meanwhile, the ability of trees to access water deeper in the soil column can support a greater latent heat flux than shallow grasses in drought (Bonan, 2008; Zaitchik et al., 2006). Thus, the greater differences in sensible and latent heat flux between trees and grasses could explain more evident daytime cooling with JWPE in dry years than in pluvial years. The subtle changes in nighttime ΔLST among different hydrological conditions suggested the variations of increased ET on nighttime warming could be tiny, as woody canopy and soil heat storage could also modify the nighttime surface temperature.

Our study area was in a semi-arid and sub-humid climate zone with mean annual precipitation (MAP) ranging from ~610 mm to 1350 mm during 2000–2015 (Fig. S4). Our results showed the daily cooling effect produced by juniper forest encroachment under various hydrological conditions of dry, normal, and pluvial years, which means that adequate soil moisture in this region can be supplied for ET cooling to offset the nighttime warming under different hydrological conditions. An afforestation study in China also showed that the regions with MAP larger than 600 mm had a stronger daytime cooing than nighttime warming, which results in a daily cooling effect of forest in grasslands (Peng et al., 2014). Thus, in terms of the precipitation-dependent spatial patterns, our results in this semi-arid and sub-humid region agrees with the previous findings of forest and grasslands on vegetation-temperature interactions (Peng et al., 2014). In this study, the comparison of the effects of juniper forest encroachment on LST among different hydrological conditions for a given region (semi-arid and sub-humid region) is complementary to the previous studies, and the findings in this study still need further verification in other climate regions such as arid and humid regions.

4.4. Implications and further studies

Climate strongly influences the geographic distribution of plant species (Foley et al., 2003). WPE can modify the local climate, which in turn affects the dynamics of woodland-grassland ecotones by regulating the feedbacks between vegetation and climate (D'Odorico et al., 2013). JWPE was found to reduce the daytime LST. This climate effect may ameliorate the drought and heat stress on the growth and productivity of juniper woody plants. Woody plants have a lower cold tolerance than grasses (Korner, 1998; Maher et al., 2005). Tree cover leads to warmer nights in their surroundings and consequently less cold stress (e.g., frost damage, freezing mortality) for seedling establishment and growth (D'Odorico et al., 2010; Langvall and Lofvenius, 2002). Such feedbacks

of daytime cooling and nighttime warming would favor woody plants to resist abiotic stress for plant survival and growth (Li et al., 2013; Maher et al., 2005). Thus, this positive feedback between JWPE and local climate could support juniper species establishment in unfavorable regions. In addition, the existence of trees would allow to maintain a certain level of humidity that could be favorable to the development of adjacent grasslands. The local climate alterations arising from WPE may have implications for large-scale climate, vegetation, carbon and water cycle, and wildlife studies.

In this study, we used satellite products to investigate the effects of juniper forest encroachment in grasslands on local surface temperature and explored two critical biophysical variables (albedo and ET). However, we have not examined the effects of JWPE on other biophysical variables such as roughness, grass types, leaf and canopy chlorophyll content of grasses due to the lack of satellite products, but such detailed studies could be considered in the future by field experiment approaches.

5. Conclusions

This study used remote sensing data to explore how local land surface temperature changed along with JWPE into the semi-arid and subhumid grasslands in Oklahoma, USA. Our results suggested that JWPE into grasslands significantly cools the local land surface in the daytime, but warms it in the nighttime. This local climate effect of JWPE in grasslands was more evident in dry years than in normal or pluvial years. Such climate effects would benefit woody plants to resist abiotic stress (e.g. drought, freezing) for survival and growth, establishing a potentially positive feedback of WPE and local climate. This study sheds some new insights to understand the WPE and climate interaction at local and large scales.

Declaration of Competing Interest

The authors declare that they have no known competing financial interests or personal relationships that could have appeared to influence the work reported in this paper.

Acknowledgments

This study was supported by the USDA National Institute of Food and Agriculture (NIFA) (2013–69002 and 2016–68002–24967), and the US National Science Foundation EPSCoR program (IIA-1301789, IIA-1920946, IIA-1946093).

Supplementary materials

Supplementary material associated with this article can be found, in the online version, at doi:10.1016/j.agrformet.2021.108508.

References

Alkama, R., Cescatti, A., 2016. Biophysical climate impacts of recent changes in global forest cover. Science 351 (6273), 600–604.
Archer, S., Vavra, M., Laycock, W., Pieper, R., 1994. Woody Plant Encroachment Into Southwestern Grasslands and savannas: rates, Patterns and Proximate causes, Ecological implications of Livestock Herbivory in the West. Society for Range Management., pp. 13–68
Archer, S.R., 2010. Rangeland conservation and shrub encroachment: new perspectives on an old problem. Wild Rangel. Conserv. Wildlife While Maint. Livest. Semi-Arid Ecosyst. (6), 53.
Barger, N.N., et al., 2011. Woody plant proliferation in North American drylands: a synthesis of impacts on ecosystem carbon balance. J. Geophys. Res-Biogeo. 116.
Betts, A.K., Ball, J.H., 1997. Albedo over the boreal forest. J. Geophys. Res-Atmos. 102 (D24), 28901–28909.
Bonan, G., 2015. Ecological Climatology: Concepts and Applications. Cambridge University Press.
Bonan, G.B., 1997. Effects of land use on the climate of the United States. Clim. Change 37 (3), 449–486.
Bonan, G.B., 1999. Frost followed the plow: impacts of deforestation on the climate of the United States. Ecol. Appl. 9 (4), 1305–1315.
Bonan, G.B., 2008. Forests and climate change: forcings, feedbacks, and the climate benefits of forests. Science 320 (5882), 1444–1449.
Bonan, G.B., Levis, S., Sitch, S., Vertenstein, M., Oleson, K.W., 2003. A dynamic global vegetation model for use with climate models: concepts and description of simulated vegetation dynamics. Glob. Chang. Biol. 9 (11), 1543–1566.
Brock, F.V., et al., 1995. The oklahoma mesonet - a technical overview. J. Atmos. Ocean Tech. 12 (1), 5–19.
Chen, B.Q., et al., 2018. Mapping forest and their spatial-temporal changes from 2007 to 2015 in tropical Hainan Island by integrating ALOS/ALOS-2L-Band SAR and Landsat Optical Images. IEEE J. Selected Top. Appl. Earth Observat. Remote Sens. 11 (3), 852–867.
Chen, J., Franklin, J.F., Spies, T.A., 1993. Contrasting microclimates among clearcut, edge, and interior of old-growth Douglas-fir forest. Agric. For. Meteorol. 63 (3), 219–237.
Christian, J., Christian, K., Basara, J.B., 2015. Drought and Pluvial Dipole Events within the Great Plains of the United States. J. Appl. Meteorol. Clim. 54 (9), 1886–1898.
D'Odorico, P., et al., 2010. Positive feedback between microclimate and shrub encroachment in the northern Chihuahuan desert. Ecosphere 1 (6).
D'Odorico, P., et al., 2013. Vegetation-microclimate feedbacks in woodland-grassland ecotones. Glob. Ecol. Biogeogr. 22 (4), 364–379.
Davin, E.L., de Noblet-Ducoudre, N., 2010. Climatic Impact of Global-Scale Deforestation: radiative versus Nonradiative Processes. J Climate 23 (1), 97–112.
Engle, D.M., Bidwell, T.G., Moseley, M.E., 1996. Invasion of Oklahoma rangelands and Forests By Eastern Redcedar and Ashe juniper. Oklahoma Cooperative Extension Service, Division of Agricultural Sciences and Natural Resources. Oklahoma State University.
Findell, K.L., et al., 2017. The impact of anthropogenic land use and land cover change on regional climate extremes. Nat. Commun. 8.
Findell, K.L., Pitman, A.J., England, M.H., Pegion, P.J., 2009. Regional and global impacts of land cover change and sea surface temperature anomalies. J. Climate 22 (12), 3248–3269.
Foley, J.A., Costa, M.H., Delire, C., Ramankutty, N., Snyder, P., 2003. Green surprise? How terrestrial ecosystems could affect earth's climate. Front Ecol Environ 1 (1), 38–44.
Foley, J.A., et al., 2005. Global consequences of land use. Science 309 (5734), 570–574.
Ge, J.J., Zou, C., 2013. Impacts of woody plant encroachment on regional climate in the southern Great Plains of the United States. J. Geophys. Res-Atmos 118 (16), 9093–9104.
Geiger, R., Aron, R.H., Todhunter, P., 2009. The Climate Near the Ground. Rowman & Littlefield.
Gibbard, S., Caldeira, K., Bala, G., Phillips, T.J., Wickett, M., 2005. Climate effects of global land cover change. Geophys. Res. Lett. 32 (23).
Grimmond, C.S.B., Robeson, S.M., Schoof, J.T., 2000. Spatial variability of microclimatic conditions within a mid-latitude deciduous forest. Clim. Res. 15 (2), 137–149.
He, Y.F., D'Odorico, P., De Wekker, S.F.J., 2015. The role of vegetation-microclimate feedback in promoting shrub encroachment in the northern Chihuahuan desert. Glob. Chang. Biol. 21 (6), 2141–2154.
He, Y.F., D'Odorico, P., De Wekker, S.F.J., Fuentes, J.D., Litvak, M., 2010. On the impact of shrub encroachment on microclimate conditions in the northern Chihuahuan desert. J. Geophys. Res-Atmos 115.
He, Y.F., De Wekker, S.F.J., Fuentes, J.D., D'Odorico, P., 2011. Coupled land-atmosphere modeling of the effects of shrub encroachment on nighttime temperatures. Agric. For. Meteorol. 151 (12), 1690–1697.
Hoagland, B., 2000. The vegetation of Oklahoma: a classification for landscape mapping and conservation planning. Southwest. Nat. 45 (4), 385–420.
Huxman, T.E., et al., 2005. Ecohydrological implications of woody plant encroachment. Ecology 86 (2), 308–319.
Jackson, R.B., Farley, K.A., Hoffmann, W.A., Jobbágy, E.G., McCulley, R.L., 2007. Carbon and Water Tradeoffs in Conversions to Forests and shrublands, Terrestrial Ecosystems in a Changing World. Springer, pp. 237–246.
Juang, J.Y., Katul, G., Siqueira, M., Stoy, P., Novick, K., 2007. Separating the effects of albedo from eco-physiological changes on surface temperature along a successional chronosequence in the southeastern United States. Geophys. Res. Lett. 34 (21).
Korner, C., 1998. A re-assessment of high elevation treeline positions and their explanation. Oecologia 115 (4), 445–459.
Langvall, O., Lofvenius, M.O., 2002. Effect of shelterwood density on nocturnal near-ground temperature, frost injury risk and budburst date of Norway spruce. For. Ecol. Manag. 168 (1–3), 149–161.
Lee, X., et al., 2011. Observed increase in local cooling effect of deforestation at higher latitudes. Nature 479 (7373), 384–387.
Li, X.Y., Zhang, S.Y., Peng, H.Y., Hu, X., Ma, Y.J., 2013. Soil water and temperature dynamics in shrub-encroached grasslands and climatic implications: results from Inner Mongolia steppe ecosystem of north China. Agric. For. Meteorol. 171, 20–30.
Li, Y., et al., 2015. Local cooling and warming effects of forests based on satellite observations. Nat. Commun. 6.
Liao, W.L., Rigden, A.J., Li, D., 2018. Attribution of local temperature response to deforestation. J. Geophys. Res-Biogeo. 123 (5), 1572–1587.
Ma, W., Jia, G.S., Zhang, A.Z., 2017. Multiple satellite-based analysis reveals complex climate effects of temperate forests and related energy budget. J. Geophys. Res-Atmos. 122 (7), 3806–3820.
Maher, E.L., Germino, M.J., Hasselquist, N.J., 2005. Interactive effects of tree and herb cover on survivorship, physiology, and microclimate of conifer seedlings at the alpine tree-line ecotone. Can J. Forest Res. 35 (3), 567–574.

Malyshev, S., Shevliakova, E., Stouffer, R.J., Pacala, S.W., 2015. Contrasting Local versus Regional Effects of Land-Use-Change-Induced Heterogeneity on Historical Climate: analysis with the GFDL Earth System Model. J. Climate 28 (13), 5448–5469.
Meneguzzo, D.M., Liknes, G.C., 2015. Status and trends of eastern redcedar (Juniperus virginiana) in the central United States: analyses and observations based on Forest Inventory and Analysis data. J. Forestry 113 (3), 325–334.
Mu, Q., Zhao, M., Running, S.W., 2013. MODIS Global Terrestrial Evapotranspiration (ET) Product (NASA MOD16A2/A3). Algorithm Theoret. Basis Document, Collect. 5.
Mu, Q.Z., Zhao, M.S., Running, S.W., 2011. Improvements to a MODIS global terrestrial evapotranspiration algorithm. Remote Sens. Environ. 115 (8), 1781–1800.
Nair, U.S., et al., 2007. Observational estimates of radiative forcing due to land use change in southwest Australia. J. Geophys. Res-Atmos 112 (D9).
Oleson, K.W., Bonan, G.B., Levis, S., Vertenstein, M., 2004. Effects of land use change on North American climate: impact of surface datasets and model biogeophysics. Clim. Dyn. 23 (2), 117–132.
Peng, S.S., et al., 2014. Afforestation in China cools local land surface temperature. Proc. Natl. Acad. Sci. U. S. A. 111 (8), 2915–2919.
Petrie, M.D., Collins, S.L., Swann, A.M., Ford, P.L., Litvak, M.E., 2015. Grassland to shrubland state transitions enhance carbon sequestration in the northern Chihuahuan Desert. Glob. Chang. Biol. 21 (3), 1226–1235.
Pitman, A.J., et al., 2009. Uncertainties in climate responses to past land cover change: first results from the LUCID intercomparison study. Geophys. Res. Lett. 36.
Qin, Y.W., et al., 2016. Mapping forests in monsoon Asia with ALOS PALSAR 50-m mosaic images and MODIS imagery in 2010. Sci. Rep-Uk 6.
Renaud, V., Innes, J.L., Dobbertin, M., Rebetez, M., 2011. Comparison between open-site and below-canopy climatic conditions in Switzerland for different types of forests over 10 years (1998-2007). Theor. Appl. Clim. 105 (1–2), 119–127.
Renaud, V., Rebetez, M., 2009. Comparison between open-site and below-canopy climatic conditions in Switzerland during the exceptionally hot summer of 2003. Agric. For. Meteorol. 149 (5), 873–880.
Running, S.W., Mu, Q., Zhao, M. and Moreno, A., 2017. MODIS Global Terrestrial Evapotranspiration (ET) Product (NASA MOD16A2/A3) NASA Earth Observing System MODIS Land Algorithm.
Saintilan, N., Rogers, K., 2015. Woody plant encroachment of grasslands: a comparison of terrestrial and wetland settings. New Phytol. 205 (3), 1062–1070.
Sankey, T.T., Germino, M.J., 2008. Assessment of juniper encroachment with the use of satellite imagery and geospatial data. Rangeland Ecol. Manag. 61 (4), 412–418.
Schaaf, C., Wang, Z., 2015. MCD43A3 MODIS/Terra+ Aqua BRDF/Albedo Daily L3 Global–500m V006. NASA EOSDIS Land Processes DAA C.
Scott, R.L., et al., 2014. When vegetation change alters ecosystem water availability. Glob. Chang. Biol. 20 (7), 2198–2210.
Shimada, M., et al., 2014. New global forest/non-forest maps from ALOS PALSAR data (2007-2010). Remote Sens. Environ. 155, 13–31.
Snyder, P.K., Delire, C., Foley, J.A., 2004. Evaluating the influence of different vegetation biomes on the global climate. Clim. Dyn. 23 (3–4), 279–302.
Spera, S.A., Galford, G.L., Coe, M.T., Macedo, M.N., Mustard, J.F., 2016. Land-use change affects water recycling in Brazil's last agricultural frontier. Glob. Chang. Biol. 22 (10), 3405–3413.
Su, Z., 2002. The surface energy balance system (SEBS) for estimation of turbulent heat fluxes. Hydrol. Earth Syst. *Sc* 6 (1), 85–99.
Villegas, J.C., Breshears, D.D., Zou, C.B., Royer, P.D., 2010. Seasonally pulsed heterogeneity in microclimate: phenology and cover effects along deciduous grassland–forest continuum. Vadose Zone J. 9 (3), 537–547.
Voicu, M.F., Comeau, P.G., 2006. Microclimatic and spruce growth gradients adjacent to young aspen stands. For. Ecol. Manag. 221 (1–3), 13–26.
Wan, Z.M., 2014. New refinements and validation of the collection-6 MODIS land-surface temperature/emissivity product. Remote Sens. Environ. 140, 36–45.
Wang, J., et al., 2017. Mapping the dynamics of eastern redcedar encroachment into grasslands during 1984–2010 through PALSAR and time series Landsat images. Remote Sens. Environ. 190, 233–246.
Wang, J., et al., 2018a. Characterizing the encroachment of juniper forests into sub-humid and semi-arid prairies from 1984 to 2010 using PALSAR and Landsat data. Remote Sens. Environ. 205, 166–179.
Wang, J., et al., 2018b. Enhanced gross primary production and evapotranspiration in juniper-encroached grasslands. Glob. Chang. Biol.
Wilcox, B.P., 2002. Shrub control and streamflow on rangelands: a process based viewpoint. J. Range Manag. 55 (4), 318–326.
Wilcox, B.P., Huang, Y., 2010. Woody plant encroachment paradox: rivers rebound as degraded grasslands convert to woodlands. Geophys. Res. Lett. 37.
Young, A., Mitchell, N., 1994. Microclimate and vegetation edge effects in a fragmented podocarp-broadleaf forest in New-Zealand. Biol. Conserv. 67 (1), 63–72.
Zaitchik, B.F., Macalady, A.K., Bonneau, L.R., Smith, R.B., 2006. Europe's 2003 heat wave: a satellite view of impacts and land-atmosphere feedbacks. Int. J. Climatol. 26 (6), 743–769.
Zhao, K.G., Jackson, R.B., 2014. Biophysical forcings of land-use changes from potential forestry activities in North America. Ecol. Monogr. 84 (2), 329–353.
Zhou, L.M., et al., 2012. Impacts of wind farms on land surface temperature. Nat. Clim. Change 2 (7), 539–543.